Paschen's law in extreme pressure and temperature conditions

G. GALLI, H. HAMRITA, C. JAMMES, M.J. KIRKPATRICK, E. ODIC, Ph. DESSANTE, Ph. MOLINIE

***Abstract*— Paschen's law gives the inception voltage for an electrical discharge as a function of the product of gas pressure and the gap distance between two infinite planar electrodes. It is known that deviations from Paschen's law occur when temperature is increased.**

Historically two theoretical corrections, the Peek and Dumbar corrections, are proposed to predict the deviation from Paschen's law by increasing temperature.

To carry out an experimental investigation on the deviation from Paschen's law by increasing temperature a customized system was designed which can operate at temperatures up to 400°C and at pressure up to 1MPa, calculated at room temperature; with an inter-electrode distance between 100µm and 6.6mm and with an error on the inter-electrode distance measurement of 20µm.

In this article, firstly, the results from the experimental investigation on the deviation from Paschen's law at temperature up to 400°C are presented. The results are then compared with theoretical corrections, and finally a theory to explain the results is proposed and discussed.

***Index Terms*—Paschen's law, argon, high temperature, high pressure.**

I. Introduction

Paschen's law gives the inception voltage for an electrical discharge in a gas as a function of the product of the gas pressure and the gap distance between two infinite planar electrodes.

The current and possible future construction of the ITER and DEMO fusion reactors, as well as the construction of sodium-cooled IVth generation nuclear reactors will necessitate the use of high temperature fission chambers [1] (HTFC) to detect neutrons in the high temperature zones of these installations [2-10]. Multiple uses are envisaged such as reactor power control and fuel cladding failure detection [11-12].To operate in–core, the HTFC will have to operate under high irradiation, up to 10^{10} n/cm².s and to withstand the high operating temperatures, up to 650°C, of the sodium-cooled fast reactors and, up to 1000°C, of the fusion reactors.

After years of study [7-10], it is now known that an electrical signal, here referred to as a partial discharge or PD, more or less similar to the signal resulting from neutron interactions, is generated in fission chambers at temperatures above 400 °C. This unwanted signal poses challenges, especially during reactor start-up when the PD signal count may be on the same order of magnitude as the neutron signal count [10].

Previous work on fission chambers [9] has focused attention on the possible implication of a solid insulator in the process leading to the creation of the unknown signal (PD). The present study considers the simplified case of a sphere-sphere geometry without any solid insulator in order to validate assumptions made in that previous work about PD activity at high temperature and pressure, and to generally enlarge the scope of the results to other fields of research.

Because of these challenges, an investigation, presented in this paper, on the effects of temperature on Paschen's law has been conducted. A brief summary of Paschen's law is described in Section II. The experimental chamber used in this work and the rest of the experimental setup are described in Section III. All results on Paschen's law in extreme pressure and temperature conditions are presented in section IV. The discussion of results with a proposed theory are presented in section V. The conclusion and the future work are presented in section VI.

II. Notions of Paschen's Law Theory

Electrical discharges are initiated when a seed electron is accelerated by an imposed electric field, acquiring energy superior to the ionization energy of the gas atoms/molecules, leading to an electron avalanche. Sources of seed electrons include cosmic rays, photo-ionization, etc.

The schema shown in figure 1 describes the basic process of an electrical discharge in a plane-to-plane geometry. Assuming

Submitted on 29 September, 2017. Work supported by the CEA, the French Alternative Energies and Atomic Energy Commission.

G. Galli is with the CEA, LIST, Sensors and Electronic Architectures Laboratory, Gif/Yvette, France and with the GeePs | Group of electrical engineering - Paris, UMR CNRS 8507, CentraleSupélec, Univ. Paris-Sud, Université Paris-Saclay, Sorbonne Universités, UPMC Univ Paris 06, 3 & 11 rue Joliot-Curie, Plateau de Moulon 91192 Gif-sur-Yvette CEDEX, France (Giacomo.GALLI@cea.fr).

H. Hamrita is with the CEA, LIST, Sensors and Electronic Architectures Laboratory, Gif/Yvette, France.

C. Jammes is with the CEA, DEN, DER, Instrumentation, Sensors and Dosimetry Laboratory, Cadarache, Saint-Paul-lez-Durance, France.

M.J. Kirkpatrick, E. Odic, Ph. Dessante and Ph. Molinie are with the GeePs | Group of electrical engineering - Paris, UMR CNRS 8507, CentraleSupélec, Univ. Paris-Sud, Université Paris-Saclay, Sorbonne Universités, UPMC Univ Paris 06, 3 & 11 rue Joliot-Curie, Plateau de Moulon 91192 Gif-sur-Yvette CEDEX, France.

the presence of a seed electron, the conditions which will lead to an electron avalanche are described by Paschen's Law (1):

$$V = A \cdot P \cdot d \cdot \frac{1}{\ln(P \cdot d \cdot B) - \ln\left(\ln\left(1 + \frac{1}{\gamma}\right)\right)} \quad (1)$$

$$A = \frac{\varepsilon_i \cdot \sigma}{k_B T} \quad (2)$$

$$B = \frac{\sigma}{k_B T} \quad (3)$$

Where P is the filling gas pressure, d is the inter-electrode distance, γ is the secondary emission coefficient (the yield of electrons from positive ion impact on the cathode which is normally on the order of 10^{-4}-10^{-2}), ε_i is the ionization potential, σ is the ionization cross section and T the gas temperature in kelvin.

Figure 1 shows the Paschen curve for argon; the product of the gas pressure and the inter-electrode distance in the abscissa and the discharge inception voltage in the ordinate. The discharge voltage passes by a minimum value on the order of a few hundred volts, depending on gas type.

Paschen's law is derived for the case of infinite planar electrodes, in other words, for the case of a homogeneous electric field.

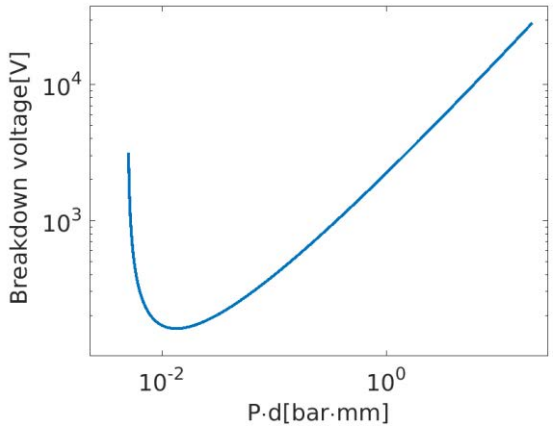

Fig. 1. Paschen curve for room temperature argon, calculated using the equations 1-3 and the values in table 2.

A. *Temperature corrections*

Two temperature corrections exist in the literature, known as the Peek and Dunbar corrections [13-14]. Both of these corrections use the ideal gas law to modify the Paschen curve. In the Peek correction, the voltage is adjusted by a factor $\frac{T_0}{T}$, lowering the curve for elevated temperatures. The Dunbar correction adjusts the pressure by a factor $\frac{T}{T_0}$, moving the curve to the right for elevated temperatures. Thus the Dunbar correction is simply the application of equations (2,3), while the Peek correction is more empirical in nature. The Dunbar correction may then be thought of as using the density instead of the pressure in the ordinate for the Paschen curve. Figure 2 compares the resulting curves calculated according to the two corrections at 400°C with the standard Paschen curve at 20°C. As seen in the figure, the two corrections have more or less the same effect of lowering the prediction for breakdown voltage at high values of Pd (on the right of the figure). These adjustments, may be understood as taking into account the fact that Paschen's law is formulated based on a mean free path for electron-neutral collisions. The mean free path for collisions is inversely proportional to the gas density, $P/k_B T$. In an open system at constant pressure, in which gas is free to expand, the gas density will decrease as a function of temperature. For a closed system like the one used in this work, it is therefore convenient to plot the Paschen curve as a function of gas density as opposed to the usual pressure. Plotted in terms of density, the uncorrected and Dunbar curves shown in Figure 2 would be seen to coincide. Therefore, for the case of a closed volume, any effect of the temperature on the breakdown voltage should appear if the data are plotted as a function of the density.

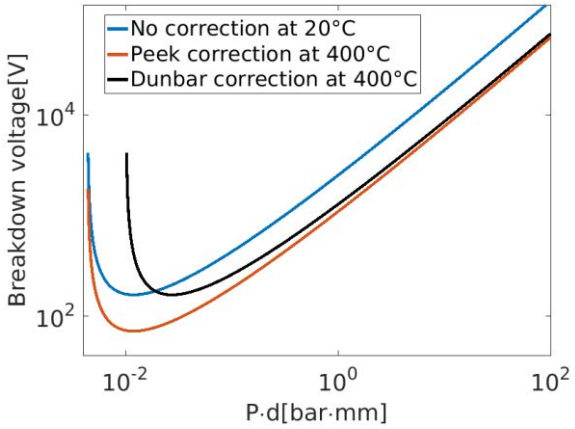

Fig. 2. Comparison of the Peek and Dunbar corrections of Paschen's law at 400 C, with the standard Paschen's curve at room temperature.

III. EXPERIMENTAL SETUP

Figure 3 shows a 3D drawing of the experimental chamber designed to test Paschen's law at high temperature and pressure. The cylindrical experimental chamber includes a gas inlet and outlet to purge the chamber and to fill the chamber with the chosen gas and two spherical electrodes in order to minimize the edge effects of the electric field and better control the inter-electrode distance. The electrodes are insulated from the chamber body by two ceramic insulators, allowing the electrodes to be polarized at voltages up to 20 kV. A micrometer screw gauge is used to adjust the inter-electrode distance.

Table 1 shows the parameters of the experimental chamber including the diameter and length, the roughness of the spherical electrodes and the electrodes diameter, and the constraints on the maximum pressure, inter-electrode distance, temperature and power supply voltage, of the experimental chamber which were specified by the fission chamber designer and then checked in the laboratory.

TABLE I
EXPERIMENTAL CHAMBER: PARAMETERS AND CONSTRAINTS

Parameters				
Chamber diameter	***Chamber length***	***Electrodes diameter***	***Electrode roughness***	***Electrode material***
75 mm	234 mm	1.6 cm	~3µm	Stainless Steel
Constraints				
P_{max}	d_{max}	d_{min}	V_{max}	T_{max}
40 bar	*6.6 mm*	*0.050 mm*	*30 kV*	*650°C*

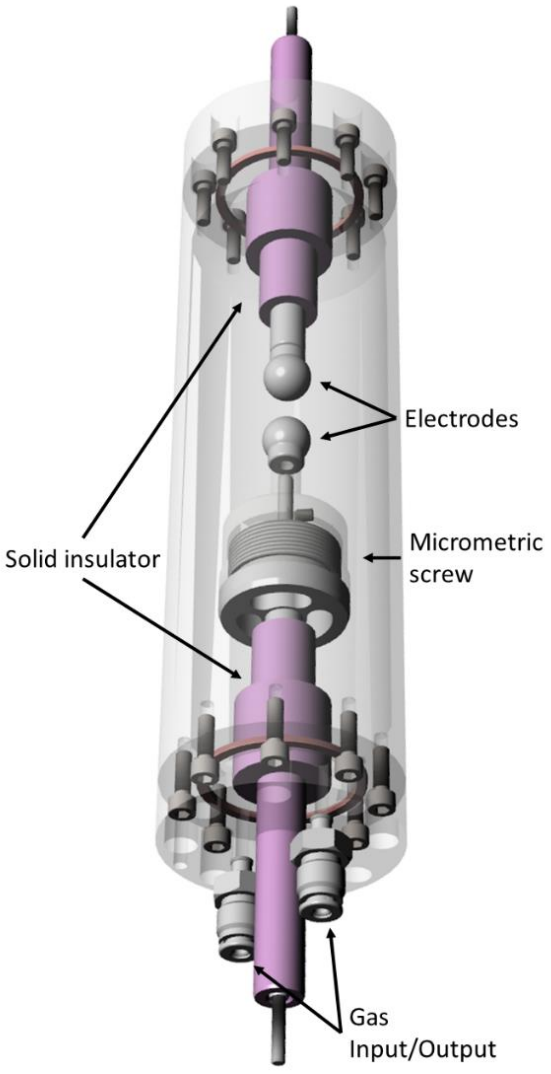

Fig. 3. 3D drawings of the experimental chamber design to test Paschen's law at high temperature and pressure.

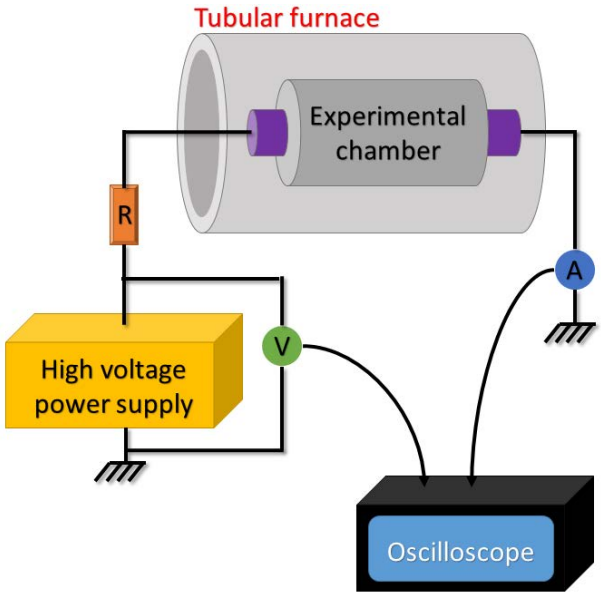

Fig. 4. Electrical schema used on Paschen's experience.

The electrode without the micrometer screw gauge in the experimental chamber was polarized by a high voltage power supply with a 100 MΩ protection resistance in series, to limit the current to avoid high currents after breakdown. The applied voltage as well as the voltage drop due to electrical discharges between the electrodes were measured using a Tektronix P6015 high voltage probe (V), connected as shown in figure 4. The discharge current (A) was measured using a Tektronix CT-1 current probe connected between the electrode with micrometer screw gauge and ground.

A. Paschen's curve as a function of the density of the gas

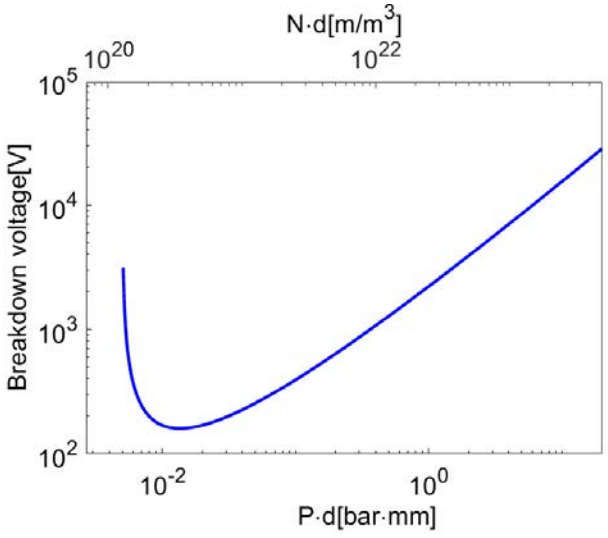

Fig. 5. Paschen's curve at room temperature in *Pd* view and in *Nd* view for argon.

As discussed above, because the experiments were performed in a closed gas volume, it was decided to plot the results of the Paschen curve not as a function of gas pressure but rather as a function of gas density, which will be constant no matter the temperature. To carry out this change of variable we have used the ideal gas law according to the formula:

$$N = \frac{P}{k_B T} \tag{4}$$

Figure 5 shows the Paschen's curves in *Pd* view and in *Nd* view where the numerical labels on the lower x-axis were transposed to those on the upper x-axis using the formula 4. From this point of the article all our results will be shown in the *Nd* view.

Paschen's law is formulated for the case where the electric field is homogeneous. To evaluate the homogeneity of the electric field in the chosen geometry for the tests, a simulation using finite elements (COMSOL) has been carried out, and is shown in figures 6 and 7.

Figure 6 shows the result, with 616 µm inter-electrode distance and 1.6 cm sphere diameter while figure 7 shows a zoom of figure 6 which better shows the distribution of the electric field.

B. *Simulation of electric field in Sphere-Sphere geometry*

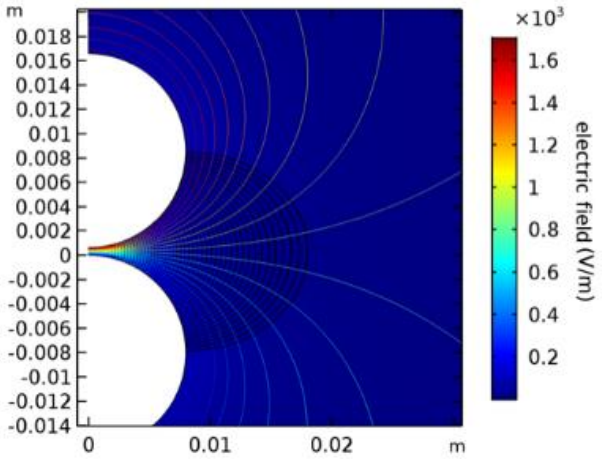

Fig. 6. Simulation of electric field, through a finite elements, in sphere-sphere geometry, with 616µm inter-electrode distance and 1.6cm sphere diameter.

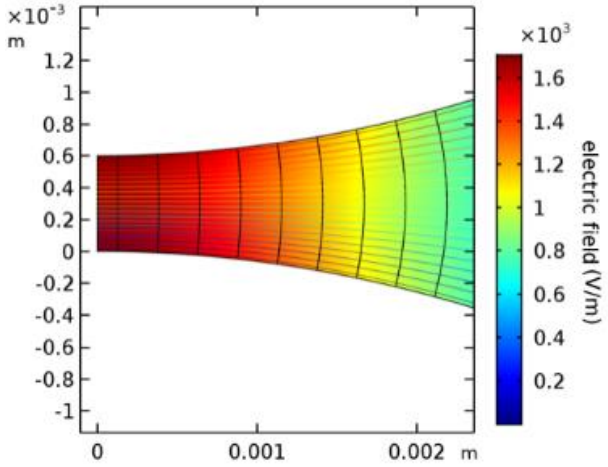

Fig. 7. Zoom of figure 6, between ±1mm in y-axis and from zero to 2mm on x-axis.

Figure 7 shows how the electric field between the electrodes is uniform axially on the center line of the spheres (between *0* and *0.0005m* radius vertical variation is less than 2%). This calculation and the fact that the experimental conditions are on the right-hand side of the Paschen curve should imply that the observed PDs were created in the shortest path region and thus in a homogeneous electric field.

C. *Change in inter-electrode distance due to material expansion caused by temperature variation*

After some tests it was clear that it was necessary to take into account the expansion of the materials in the experimental chamber due to the temperature change. The expansion was found to significantly affect the inter-electrode distance. To solve this challenge, calculations were made based on linear expansion of the various components making up the chamber.

To verify these calculations, the following test was made: the inter-electrode distance was adjusted to a known value at room temperature. The experimental chamber was then placed in a climate-controlled device which could cool the chamber down as low as -50°C and contact between the electrodes was measured using a multimeter.

Figure 8 shows the variation of the inter-electrode distance as a function of the temperature variation calculated based on the chamber geometry and materials (blue line), and the experimental tests for contact of the electrodes when cooling the chamber (red points). The tests may be seen to verify the calculation. The calculation of the inter-electrode distance variation with temperature will therefore be used in the following section to correct the inter-electrode distance.

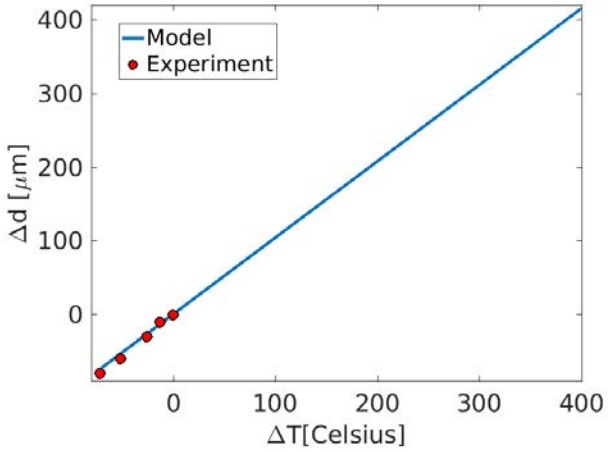

Fig. 8. Variation of inter-electrode distance as a function of the temperature variation calculated using a model, based on the linear expansion taking into account the complete geometry of the experimental chamber as well as the different materials involved, (blue line) and the experimental points obtained through laboratory tests (red circles).

IV. Paschen's law temperature effects: results and experimental uncertainties

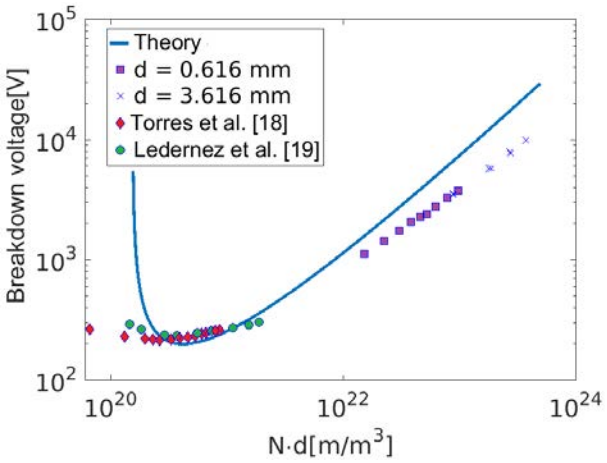

Fig. 9. Paschen's curve for argon at room temperature (blue line) and experimental points on Paschen's curve obtained by varying the gas density in the experimental chamber at room temperature with two inter-electrode distances.

Using the tube furnace as seen in the schema in figure 4, the temperature of the chamber was adjusted and measured by two thermocouples, one placed in contact with the chamber exterior and the other inside the furnace itself. The applied voltage was then increased until detection of a discharge via the current and voltage measurements. Each experimental point was obtained several times, so that for each point, the experimental uncertainty could be calculated, which will also be shown in figure 11 and table 3.

Firstly, the points on Paschen's curve were obtained at room temperature in order to test the experimental chamber and to have some room temperature reference points.

TABLE 2
PARAMETERS OF PASCHEN'S LAW FOR ARGON [15] [16] [17]

ε_i	σ	T	γ
$2.524 \cdot 10^{-18} J$	$3 \cdot 10^{-20} m^2$	$298\ K$	$2.5 \cdot 10^{-2}$

Figure 9 shows the theoretical Paschen curve calculated according to equation 1, using the values in table 2. Also shown are two series of experimental points, at room temperature, obtained for two different inter-electrode distances with the experimental chamber and two series of experimental points found in the literature [18-19].

Figure 9 shows also that the experimental points from this work in addition to experimental points found in the literature deviate slightly from the theoretical Paschen's curve because, especially for argon, the theoretical Paschen's curve is a good but not perfect approximation of reality. In this specific case then, in the used formula (eq. 1), the secondary emission coefficient (γ) is an approximation of the real one, because it takes into account only the positive ion impact on the cathode.

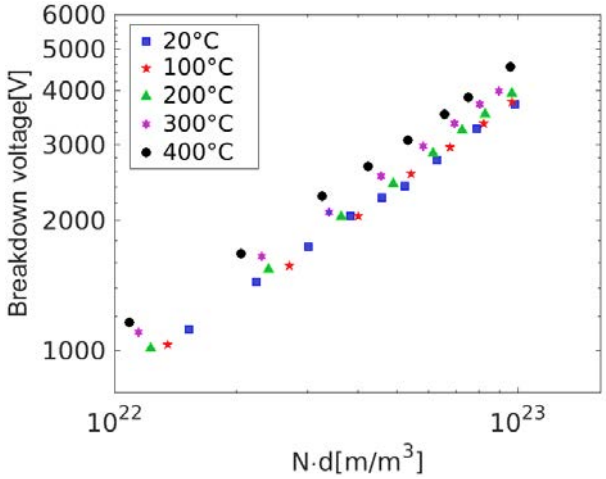

Fig. 10. Results on temperature effect, from 20 C to 400 C, of the breakdown voltage for argon.

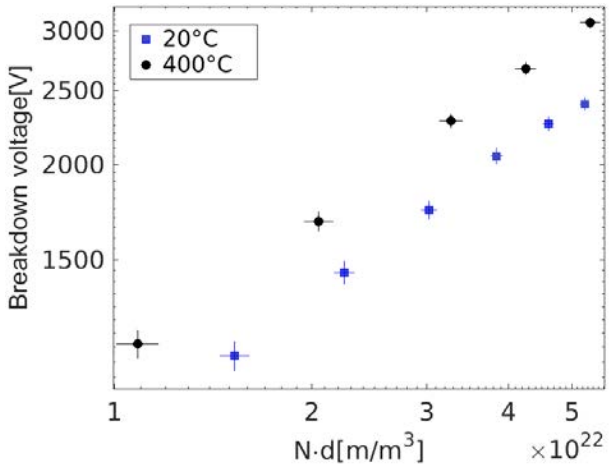

Fig. 11. Results on the effect of increasing temperature on the breakdown voltage for argon, with error bars, at room temperature (blue squares) and at 400 C (black circles).

It should be noted at this point that for all experiments, the experimental chamber was purged three times by pumping down to 1mbar and then refilling to 8bar with argon, so as to eliminate as much as possible the sources of uncertainty on the composition of the gas inside the experimental chamber (outgassing of material inside the experimental chamber with temperature). For the experiments at elevated temperature, these purges were made after the temperature of the chamber had stabilized at the target temperature, and so any gas desorbed from the chamber walls should have been replaced by fresh argon.

Figure 10 shows the results when increasing temperature from 20°C to 400°C, of Paschen' law for argon, in which it is observed that an increase in temperature leads to an increase in the breakdown voltage. This was confirmed by experiments being repeated at low temperature after heating; these experiments gave the same results before and after heating and thus eliminated the possibility of hysteresis effects.

Table 3 shows the measurement uncertainties: for the inter-electrode distance, pressure, and temperature, the uncertainty depends on the measuring instruments and for the breakdown voltage the uncertainty was calculated as the standard deviation of several tests.

Figure 11 shows some of the same data from Figure 10 while zooming in and adding the error bars, calculated starting from the uncertainty values listed in Table 3.

TABLE 3
EXPERIMENTAL CHAMBER: PARAMETERS AND CONSTRAINTS

$T \leq 25$℃			
d [μm]	***V [Volt]***	***T [K]***	***P [mbar]***
± 10	± 50	± 1	± 50
$T > 25$℃			
d [μm]	***V [Volt]***	***T [K]***	***P [mbar]***
± 25	± 50	± 1	± 50

V. DISCUSSION OF RESULTS WITH PROPOSED THEORY

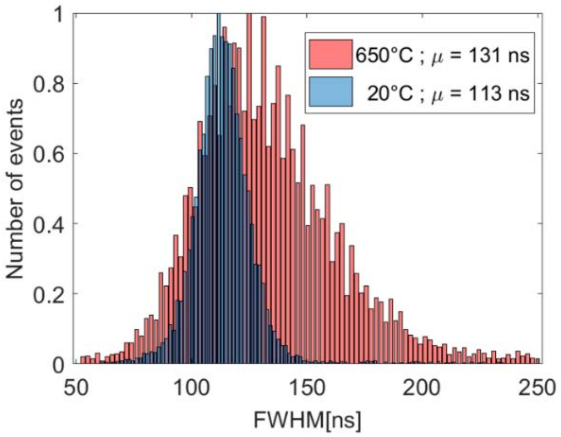

Fig. 12. Histograms of full width at half maximum, at 20 C (blue) and at 650 C (red), of the pulses created by a fission chamber, filled with argon at 3.5 bar.

The Dunbar and Peek corrections, both intended for use in the situation of a gas which is free to expand, logically give a decrease of breakdown voltage for an increase in temperature, due to the gas density decrease. The experiments in this work indicate that, at constant gas density, an increase in temperature leads to an increase in breakdown voltage.

To explain this result, it is proposed that the Maxwell distribution and corresponding drift velocity is shifted downward for increasing temperatures, which is true for argon ions in the argon itself [20]. Figure 13 shows a given Maxwell distribution of the free electrons velocities and drift velocity; the population of energetic electrons which are involved in ionization and therefore to breakdown. If the distribution shifts to the left as shown in Figure 13, the critical density of free energetic electrons may be insufficient to initiate a detectable breakdown, and therefore a higher applied voltage will be needed to observe breakdown. But when we increase the temperature we know, using the fission chamber experiences results in figure 12, drift velocity shifts to smaller values and the velocity distribution is modified accordingly, in this way we can imagine that the density of electrons responsible for the avalanche (n_A) decreases enough to extinguish the phenomenon of discharge, therefore the only way to re-ignite the discharge phenomenon is an increasing in the voltage power supply in way to restore the required value of the electron density responsible for the avalanche.

There are many examples in the literature of how the drift velocity of free electrons decreases with increasing temperature in solid insulators, but the analogy to a gas is not trivial. In order to investigate this idea, a fission chamber [1] was used, filled with argon at 3.5 bar, in which full width at half maximum (FWHM) of the pulses is inversely proportional to the drift velocity of the free electrons in the gas. In the experiment pulses were recorded using one fission chamber irradiated by the same neutron flux at 20°C and at 650°C, and the FWHM of each pulse was calculated in order to get information on the variation of FWHM as a function of temperature.

Figure 12 shows the histograms of FWHM, at 20°C and at 650°C, of the pulses created by the same fission chamber, filled with argon at 3.5 bar. Figure 12 shows also how increasing temperature leads to an increase of the mean FWHM; this indicates a decrease of the drift velocity of free electrons.

This phenomenon can be explained (drawing a parallel with the temperature effects on the drift velocity of the electrodes in a conductor) by the following reasoning: in a closed gas volume, the mean free path of electrons is constant but the average time between collisions decreases with increasing temperature and this increased collision frequency causes the decrease of the drift velocity of free electrons.

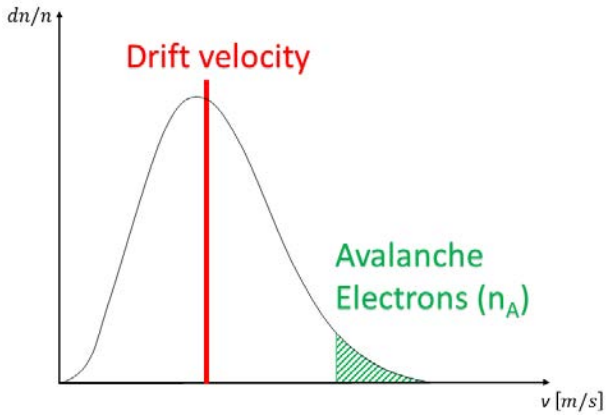

Fig. 13. Schema of Maxwell distribution of free electrons in gas with details with regards to the drift velocity and the density of free electrons responsible for the avalanche.

VI. CONCLUSION AND FUTURE WORK

In this article results were presented on the effect of temperature Paschen's law for argon, in a closed gas volume. It was observed that breakdown increases with increasing temperature at a fixed gas density. A theory, supported by experimental results, has been proposed to explain this phenomenon.

Future work will consider other values for the inter-electrode distance as well as different electrode geometries, which will be tested also in the presence of a ceramic insulators, to look for the effects of temperature on a triple point, metal-gas-solid insulator. Finally, different gases as well as gas mixtures, such as argon plus nitrogen, because of their wide use in the nuclear sensor industry, will be tested.

REFERENCES

[1] G. F. Knoll, *Radiation Detection and Measurement*, Wiley, New York, 1989.

[2] S. Andriamonje *et al.*, "New neutron detector based on micromegas technology for ADS projects", *Nuclear Inst. and Methods in Physics Research, A*, vol. 562, Issue 2, 2006.

[3] B. Geslot *et al.*, "Development and manufacturing of special fission chamber for in-core measurement requirements in nuclear reactor", *in Proceeding of the First International Conference on Advancements in Nuclear Instrumentation Measurement Methods and their Applications (ANIMMA)*, France, 2009.

[4] C. Jammes *et al.*, "Advantage of the area-ratio pulsed neutron source technique for ADS reactivity calibration", *Nuclear Inst. and Methods in Physics Research, A*, vol. 562, Issue 2, 2006.

[5] C. Jammes *et al.*, "Comparison of reactivity estimations obtained from rod-drop and pulsed neutron source experiments", *Annals of Nuclear Energy*, vol. 32, Issue 10, 2005.

[6] C. Jammes *et al.,* "Assessment of the high temperature fission chamber technology for the French fast reactor program", *IEEE Trans. Nucl. Sci*., vol. 59, n. 4, 2012.

[7] J. P. Trapp *et al.*, "High Temperature Fission Chambers: State-of-the-Art", *In-Core Instrumentation and Reactor Core Assessment. Proceedings of a Specialist Meeting*, Japan, 1996.

[8] H. Hamrita *et al.*, "Rejection of partial-discharge-induced pulses in fission chambers designed for sodium-cooled fast reactors", *Nuclear Inst. and Methods in Physics Research, A*, vol. 848, pages. 109-113, 2017.

[9] G. Galli *et al.*, "Characterization and localization of partial discharge-iduced pulses in fission chambers designed for sodium-cooled fast reactors", *IEEE Transactions on Nuclear Science*, vol. 65, Issue 9, 2018.

[10] C. Jammes *et al.*, "Progress in the development of the neutron flux monitoring system of the French GEN-IV SFR: simulations and experimental validations", *Proceeding in ANIMMA*, 2015.

[11] C. Blandin *et al.*, "Development and modeling of neutron detectors for in-core measurement requirements in nuclear reactors", *Proceeding in 10th International Symposium on Reactor Dosimetry*, 1999.

[12] C. Jammes *et al.*, "Research Activities in Fission Chamber Modeling in Support of the Nuclear Energy Industry", *IEEE Transactions on Nuclear Science*, vol. 57, n. 6, 2010.

[13] F.W Peek, "Phenomenes Dielectriques dans la technique des Hautes Tensions", Traduction par R. Ackerman, Delagrave Editions, Paris, 1924.

[14] W. Dunbar, "High Voltage Design Guide for Airborn Equipment", Boeing Aerospace Company, Seattles ADA029268, 1976.

[15] D. R. Lide, "CRC Handbook of Chemistry and Physics", 87e éd., 2006

[16] R. Udiljak *et al.*, "Improved model for multipactor in low pressure gas", Physics of plasmas, vol. 11, n. 11, 2004.

[17] Z. Donko, "Apparent secondary-electron emission coefficient and the voltage-current characteristics of argon glow discharges", Physical review E, vol. 64, 2001.

[18] Torres *et al*.., "Paschen law for Argon glow discharge", *Proceeding in LAPWPP*, 2011

[19] L. Ledernez *et al*., "A modification Paschen law for argon", *Proceeding in ICPIG*, 2009.

[20] L. M. Chanin *et al.*, "Temperature Dependence of Ion Mobilities in Helium, Neon, and Argon" Physical review, vol. 106, n. 3, 1957.